Inorganica Chimica Acta xxx (xxxx) 121268

Contents lists available at ScienceDirect

Inorganica Chimica Acta

journal homepage: www.elsevier.com/locate/ica

Novel Synthesis of Zinc Oxide Nanoparticles from Type IV Deep Eutectic Solvents

Lorenzo Gontrani [a,*], Domenica Tommasa Donia [b], Elvira Maria Bauer [c], Pietro Tagliatesta [a], Marilena Carbone [a,*]

[a] Department of Chemical Science and Technologies, University of Rome "Tor Vergata", Via della Ricerca Scientifica 1, 00133 Rome, Italy
[b] Department of Surgical Science, University of Rome Tor Vergata, Via Montpellier 1, 00133 Rome, Italy
[c] Italian National Research Council-Institute of Structure of Matter (CNR-ISM), Via Salaria km 29.3, 00015 Monterotondo, Italy

ARTICLE INFO

Keywords:
Metal Deep Eutectic Solvents
Nanoparticles
Inorganic synthesis
Type IV DES
Layered nanoparticles
Zinc Oxide

ABSTRACT

One of the fields where DES show remarkable added-values is the synthesis of inorganic materials, in particular nanoparticles. In this field, the inherent and highly-tunable nano-homogeneities of DES structure give origin to a marked templating effect, a precious role that has led to the recent bloom of a vast number of studies exploiting these new synthesis media to prepare nanomaterials and composite structures of various kinds. In this contribution, three examples of synthesis of nanoparticles containing zinc, using metal type-IV Deep Eutectic Solvents, a pathway that has never been explored so far, is described. The prepared materials have layered shapes, and when zinc nitrate is used as DES component, pure layered ZnO is obtained, forming nanometric platelets that assemble to form flower-like aggregates. The prepared nanoparticles show intrinsic fluorescence, and are being further studied to set up sensors for the detection of various contaminants.

1. Introduction

Zinc oxide (ZnO) is one of the inorganic compounds that have recently gained the largest popularity, owing to the opto-electronic properties it possesses notwithstanding the relatively low cost, such as wide band-gap and high exciton binding energy (3.35 eV and 60 meV, respectively), piezoelectricity and intrinsic fluorescence [1–3]. These features are highly desirable in several materials science fields and their exploitation has led to a quite wide range of devices, like UV light emitting diodes [4], UV lasers [5], gas sensors [6], photo-catalysts [7], supercapacitors [8] and photovoltaic devices [9–12]. In addition, ZnO has found several applications in environment-related domains, as in the photocatalytic degradation of contaminants [13], in the use as biocide or as nanofertilizer in crop growing [14,15]. As it occurs quite often with several types of nanomaterials and more specifically with metal oxides, the properties are highly dependent on the microscopical structural properties and on the morphology of the molecules [16–24].

Overall, the synthetic strategies to obtain ZnO should consequently take care of both aspects, namely they should lead to nanoparticles of the desired size/shape at low cost and low environmental impact. Several reports claiming the use of "green" room temperature conditions that succeeded in pursuing these sustainability goals can be found in the recent literature, and are reviewed in Donia et al. [25]. In the same paper, a synthetic pathway using mild and ''green'' conditions with water as reaction medium and low temperatures for the oxide formation and drying is reported, with the added value of controlling the nanoparticles dimension by a simple control of the latter ones. In particular, it was found that a minimum temperature of 40 °C was needed to obtain pure ZnO thus avoiding the co-presence of the hydroxide $Zn(OH)_2$, and that an increase in temperature led to particles of larger size. A still quite non-ordinary method concerns the use of Deep Eutectic Solvents (DES), a research strand in the field of nanoparticle synthesis that has been blossoming for the last few years, with a very large amount of investigations reported (several hundreds from 2020 until

DES Deep Eutectic Solvents, NP Nanoparticles; HBD Hydrogen Bond Donor, HBA Hydrogen Bond Acceptor; LADES Lewis Acidic DES, LDH Layered Double Hydroxide; LHS Layered Hydroxide Salts, ZHS Zinc Hydroxide Salts; SEM Scanning Electron Microscopy, UV Ultraviolet; BADES Brønsted Acidic DES, XRD X-Ray Diffraction

* Corresponding authors.
E-mail addresses: lorenzo.gontrani@uniroma2.it (L. Gontrani), carbone@uniroma2.it (M. Carbone).

[1] Special Issue: "Claudio Pettinari: a protagonist in Inorganic Chemistry"

https://doi.org/10.1016/j.ica.2022.121268
Received 15 June 2022; Received in revised form 22 September 2022; Accepted 20 October 2022
0020-1693/© 20XX

now). This topic has been reviewed in some recent articles [26–29], and was the subject of a recent work by some of us [30].

These innovative materials gather several outstanding features, like the simplicity of the preparation, their lack of toxicity, biocompatibility, but most importantly, along with these coveted aspects, DES are characterized by an intrinsic inhomogeneity in their structure that can be traced back to the filling of anions' coordination shells and to the microsegregation of domains of different polarity [31–36], as well as to the presence of holes in the structure [37]. All these features can result in a marked templating effect which imparts peculiar shapes to the product nanoparticles. In this contribution, we focus our attention on systems belonging to an almost unexplored variant of Deep Eutectic Solvents, namely LADES (Lewis Acidic DES) that are obtained by the simple mixing of metal salts (like chlorides, nitrates, triflates, often hydrated) with hydrogen bond donors (HBD) such as urea or acetamide. This family of compounds differs from other more common DES obtained by mixing choline chloride or another similar quaternary ammonium cation as hydrogen bond acceptor (HBA) [38] with Brønsted acids acting as hydrogen-bond donors, like, e. g. carboxylic acids. Such compounds could be termed as "BADES" (Bronsted Acidic DES) and belong to "Type III" in the seminal paper on DES classification by Abbott et al. [39], whereas LADES containing electrophilic metal cations and urea or similar HBD systems are termed "Type IV" DES.

By using LADES, the metal source necessary for the synthesis is introduced in the system directly as a component of the DES mixture, at variance with the more common procedures, where the metal salt is added to a previously formed liquid system, as it occurs, for instance, when metal oxides are solubilized in the protypical DES reline (the mixture choline chloride:urea at 1:2 M ratio, a type III DES) to perform, for instance, the electrodeposition of the metal or oxide [40–42], to synthesize composite systems [43–45] or directly nanoparticles [46–48]. Among the few examples of LADES reported, the majority of the studies deal with chloride salts, like ChCl:2$ZnCl_2$, ChCl:2$CrCl_3{\cdot}6H_2O$ and $ZnCl_2$:urea melts [49–51]. The last type of mixtures have been reported to produce homogeneous and transparent liquid phases in a wide range of $ZnCl_2$:urea compositions (ranging from 2.5 to 4.5:10) and temperatures, and have glass to liquid transition temperatures (measured by DSC experiments) as low as −20 °C [52], though in Abbott et al. work dedicated to metal-containing eutectics the lowest freezing temperature (-9°C) was observed for 1:3.5 mixtures [53]. Few examples of mixtures of different types were reported, like some nitrate-amide eutectics [54], such as $LiNO_3$:acetamide 22:78 (1:3.54), which was recently employed within electrochemical capacitors [55] and silver triflate:acetamide 1:4 (''argentous'' DES [56]), that was proposed to obtain silver nanocrystals in large quantities.

In this work, we aimed at testing the different behaviour of three commonly available zinc(II) salts, namely zinc chloride, zinc nitrate hexahydrate and zinc acetate dihydrate, in obtaining a (DES) liquid phase by mixing them with urea in the 22:78 M ratio already used in $ZnCl_2$:urea and $LiNO_3$:acetamide studies referenced above, and in employing the latter liquid as reaction medium for the precipitation of zinc hydroxide $Zn(OH)_2$ / zinc oxide ZnO upon reaction with equimolar quantities of NaOH (2 mol of NaOH per moles of zinc), with the final goal of obtaining ZnO directly or after drying the hydroxide in mild conditions. Actually, the urea:anion ratio (i. e. urea:chloride, urea:nitrate and urea acetate) used in this study, namely 3.54:2 = 1.57 urea per anion - since all the salts contain divalent zinc cations and have the general formula Zn:X2, X = anion) – is slightly smaller than the analogous ratio in the prototypical DES reline (urea:choline chloride 2:1 = 2 urea per chloride anion). Regarding the precipitation of zinc as hydroxide or oxide, several studies have shown that different types of zinc salts can be obtained by precipitation at basic pH, depending on the conditions and on the choice of the salt anion. Indeed, zinc has a marked tendency of forming hybrid layered materials like Layered Double Hydroxides (LDH, [57]) or Layered Hydroxide Salts (LHS) [58]. The first family of materials, of general formula $[M^{2+}_{1-x}M^{3+}_{x}(OH)_2]^{x+}(A^{m-})_{x/m}{\cdot}nH_2O$, consists of layers of octahedral ions possessing a brucite-like structure where the divalent metal ions (M^{2+}) are partially substituted by trivalent cations (M^{3+}), with anion and/or water molecules occupying the interlayer space and balancing the positive charge. In absence of trivalent cations, instead, it becomes possible to form LHS, of general formula $M^{2+}(OH)_{2-x}(A^{m-})_{x/m}{\cdot}nH_2O$. More specifically, Zinc Hydroxy Salts (ZHS) can be synthesized. In such type of layered material, four octahedral sites are not occupied by Zn^{2+} ions, which are placed, instead, in tetrahedral sites below and above each empty octahedron. Furthermore, three OH– groups make up the base of the tetrahedron, whereas a water molecule is coordinated on its apex. Among ZHS compounds, relevant to our study are zinc hydroxy chloride (ZHC) [59], zinc hydroxy nitrate (ZHN) [59] and zinc hydroxy acetate (ZHA) [60]. Powder XRD of these compounds have been reported; furthermore, the structure of crystalline ZHC, found in mineral Simonkolleite, was investigated by single-crystal X-ray diffraction [61] and by infrared spectroscopy. [62,63]. All the former diffraction profiles show the presence of intense peaks at low angles ($2\theta \leq 10°$ using Cu radiation), that are typical fingerprints originated by the correlation distance between planes of the layered structure. A related issue influencing the precipitation of zinc oxide/hydroxide is the co-presence of chlorine/chloride moieties, for which zinc cations show large affinity, in the starting reactant mixture/solution. Actually, it has been known for some time [64,65] that the dissolution of $ZnCl_2$ in water leads to the formation of oxychloride (ZnClO) complex species, and a similar behaviour has been noticed in DES as well in recent studies [66,67], which point out that the dissolution of ZnO in choline chloride:urea 1:2 (reline, ChCl) leads to the establishment of [ZnClO···urea] aggregates, whereas in the Type-IV DES $ZnCl_2$:urea 1:3..5, i. e. one of the three mixtures considered here for ZnO nanoparticle synthesis, complex polychloro zincate anions like $[ZnCl_3]^-$, $[Zn_2Cl_5]^-$ and $[Zn_3Cl_7]^-$ as well as $[ZnCl]^+$ based cations like $[ZnCl(urea)]^+$, $[ZnCl(urea)_2]^+$ and $[ZnCl(urea)_3]^+$ were found [53]. In a preliminary test performed in our lab before considering the use of LADES we tried to precipitate ZnO from a 0.1 M $Zn(NO_3)_2$ Reline solution, by adding solid NaOH, but the flower-like nanoparticles obtained (see supporting information) turned out to have the quite complex composition $C_{30}Cl_1Zn_7O_{28}$.

All the nanoparticles obtained by precipitation in DES were dried and characterized by infrared spectroscopy (IR), powder X-ray diffraction (XRD) and scanning electron microscopy (scanning electron) (SEM) . The results were compared with crystal phase data and with infrared spectra, where available. Finally, an additional photoluminescence study of the synthesized NPs was carried out, in order to assess the effect of the observed morphologies on the emitted light.

2. Experimental

2.1. Synthesis

2.1.1. DES preparation

After performing preliminary test on minimal quantities, 2 g of each of the following mixtures were prepared by weighing the appropiate quantities of the two components, according to the 1:3.54 salt:urea molar ratio:

$ZnCl_2$: urea ("ZCD1", , negative control).

$Zn(NO_3)_2$:urea ("ZND1").

$Zn(CH_3COO)_2$:urea ("ZAD1").

The weighted quantities were promptly transferred into sealable vials, in order to minimize humidity absorption. When the two components were put in contact, in the first two systems (ZCD1 and ZND1) a sluggish translucent agglomerate was formed quite rapidly, which become more fluid and transparent upon gentle heating and stirring (35–40 °C, 600 rpm) and remained liquid at room temperature (around 15–20 °C, see Fig. 1). As concerns ZAD1, the liquid phase was formed at

Fig. 1. Liquid ZND1 at room temperature.

significantly higher temperature (after 80–85 °C) and the solid phase was rereobtained immediately when the heating plate was switched off. The solidification of ZDA1 was favoured by the glass container, especially if it was stretched with a glass stick. In any case, the formation of water drops on the vial walls was noticed, probably coming from the absorbed humidity or, possibly, from a partial desorption of crystallization water molecules.

2.1.2. Precipitation reaction with sodium hydroxide

Equimolar quantities of solid NaOH (two moles of NaOH per mole of zinc), finely powdered in advance in a mortar, were weighted and added to the "hot" liquid mixtures under stirring. The temperatures chosen were 60 °C and 85 °C for ZCD1/ZND1 and ZAD1, respectively. A pearly precipitate appeared after few minutes, and the system was let react for 20 min. In ZCD1, evolution of ammonia from the precipitate was detected from the typical odour. The precipitate was washed with 20 mL of distilled water at least four times and centrifuged for 5 min at 3000 rpm after each rinse cycle. The washing procedure was stopped when pH 7 was reached, signaling that the excess amounts of NaOH and urea had been washed out.

2.1.3. Drying

The washed precipitate was collected from the vial and dried around 40 °C in the open air, as in our "green" synthesis method recently reported [25]. Water evaporation process was accompanied by a change in the physical appearence of the system, that passed from "shaving foam" to flaky consistency. The flaky appearence was more pronounced for the powder obtained using $Zn(NO_3)_2$:urea DES.

2.1.4. Instrumentation

The samples were analyzed in a Field Emission Microscope Zeiss Auriga 405, 1 nm nominal resolution (Oberkochen, Germany), mounting a Gemini column and operating at 7 kV and equipped with a Bruker Quantax energy dispersive X-ray spectroscope (Energy Resolution: 123 eV Kα of the Mn). Samples were observed under high vacuum (10^{-5}–10^{-6} mbar). The microanalysis, which allows the quantitative determination of the chemical elements present in the sample, was carried out at an increasing accelerating voltage E_0 = 3, 5, 10, 15 keV. Given the relationship between the accelerating voltage and the penetration, x = 0.1 E_0 1.5/r (r = 4.75 g/cm^3), experiments at variable E_0 allowed us to obtain a qualitative determination of the profile of the composition.

Images were recorded on both fine powders precipitated from a drop of water dispersions of the sample (drop-cast method) and on small portions of the solid.

XRD patterns were collected in transmission geometry with an X'pert pro X-ray diffractometer by Philips, using Cu Kα (λ = 1.5407 Å). The measurements for each sample were repeated to get the accuracy in the results and to check if there was any damage/degradation in the structure due to radiation but the results were the same in all cases. Primary data were processed performing the necessary corrections for the background and sample absorption, and the scattered intensity I_{EXP} was obtained. All the diffraction patterns were analyzed by a Rietveld procedure with the GSAS-II suite of programs [68]. Infrared spectra were recorded with a Shimadzu Prestige-21 FT-IR instrument, equipped with an attenuated total reflectance (ATR) diamond crystal (Specac Golden Gate), in the range 400–4000 cm^{-1}, with a resolution of 4 cm^{-1}.

Photoluminescence (PL) excitation and emission measurements were performed using a JASCO FP-8500 spectrofluorometer, equipped with a 150 W xenon lamp as the source of excitation, operated both in excitation and emission mode, with em and ex slits both set at 5 nm The emission spectra of 1 mg/mL ethanol dispersions of the synthesized solid samples were recorded at 330 nm excitation wavelength. The liquids (dispersions and pure solvent) were contained in quartz cuvettes of 1 cm optical length. The final PL spectrum of each sample was corrected for the background luminescence of the pure solvent (ethanol), by subtraction.

3. Results and discussion

3.1. Characterization of ZCD1

The measured XRD spectrum of solid ZCD1 is reported in Fig. 2, top. The structure of the particles obtained confirm the prediction regarding the easy formation of oxychloride salts when Cl atoms (or ions) are present in the solution. Actually, the XRD profile could be satisfactorily fitted within the

Rietveld method in the range 10–90° 2θ, using the reflections measured in the crystal structure of Simonkolleite mineral, a Layered Hydroxy Salt having brutto formula $Zn_5(OH)_8Cl_2(H_2O)$. The crystal structure data of this LHS system are a = 6.334 Å, c = 23.58 Å, Z = 3;

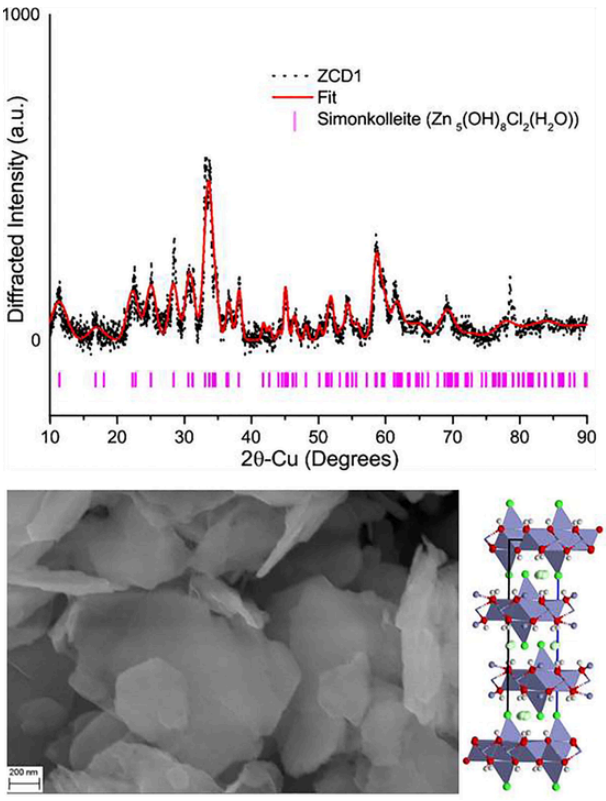

Fig. 2. ZCD1 PXRD spectrum (top panel), sample SEM image (bottom panel, left), Simonkolleite layered crystal structure (bottom panel, right).

V = 819.28 Å^3, accounting for the large separation between the layers (c axis); the calculated density is 3.36 g cm^{-3} and the space group is *R*-3 m (rhombohedral with hexagonal axes). A sketch of the crystal is shown in Fig. 2, bottom panel (right). Once fitted in the nanoparticle system, these parameters were refined to a = 6.31803 Å, c = 23.60071 Å V = 815.866 Å^3, with calculated density = 3.383 g cm^{-3} The SEM images taken from the drop-cast solid show the presence of aggregates of platelets containing hexagonal nanoparticles of variable dimensions, ranging from 100 to 800 nm. The microanalysis performed on these SEM images, reported as additional material, shows the evident presence of chlorine, compliant with a LHS containing Cl like Simonkolleite. The infrared spectrum of ZCD1, reported in Fig. 3, bottom (black line), was compared with that of solid Simonkolleite [62] and with the patterns of the two DES precursors $ZnCl_2$ [69] and urea. The similitude with the mineral spectrum is high in the 500–1200 cm^{-1} range, while new features appear beyond, namely in the 1400–1600 cm^{-1} range, and, most remarkably, at 2282 cm^{-1}, where an evident peak appears. Owing to these features and ruling out the presence of unreacted $ZnCl_2$ and urea, given the lack of correspondence between peaks, the spectrum could be reasonably assigned to traces of DES co-precipitated with the oxychloride. Indeed, in a recent study on $ZnCl_2$:urea 1:3.5 DES Solorzano et al. [69] described the presence of a peak at 2224 cm^{-1} that was assigned to coordination bonds between urea carbonyl group and zinc (chloride), with the concomitant marked red-shift of urea C═O stretching down to 1622 cm^{-1}; the peaks falling the 1500–1400 cm^{-1} range were attributed to N—H and C—N bending normal modes. Noteworthy, the presence of this contamination in ZCD1 could not be evidenced in the analysis of XRD spectrum, probably owing to the amorphous nature of the solid, whose diffraction contribution was buried in the background.

4. Characterization of ZND1

The measured XRD spectrum of solid ZND1 is reported in Fig. 4. The pattern contains few peaks in the range 10–90° 2θ, and is the typical spectrum of pure hexagonal ZnO, containing the central intense "triad peaks" at 31.8, 34.4 and 36.3°, corresponding to [1,0,0], [0,0,2] and [1,0,1] reflections. The pattern was very well fit with Rietveld method using the published zincite structure [70], which is shown in the right part of the bottom panel of Fig. 4. The fitted parameters were a = 2.92027 Å, c = 5.21949 Å, V = 38.548 Å^3, density = 7.011 g cm^{-3}, space group P 63 m c. With respect to zincite crystal data reported in the database (a = 3.2495 Å, c = 5.2069 Å, V = 47.615 Å^3, d = 5.676 g cm^{-3}, the obtained nanoparticles are predicted to have a stretched a axis and larger density, though this could well result from parameters overfitting. The SEM images, reported in Fig. 4, show that the powder is composed of layered nanoplatelets with longer dimension around 100 nm and smaller dimension around 10 nm (estimated). The nanoparticles form flower-like assemblies with dimensions extending up to 5–10 μm (see lower magnification images in the supporting information). The EDX microanalysis of SEM images (see supporting information, Fig. S2) showed that the nanoparticles contained only zinc and oxygen atoms with corresponding ZnO composition whereas the inspection of ZND1 infrared spectrum, which is reported in Fig. 5 overlayed with the patterns of the two precursors (zinc nitrate hexahydrate and urea) confirmed the high purity of the obtained solid. Actually, the plot shows only very small traces of absorbed humidity (OH stretching band around 3400 cm^{-1}) and negligible contributions from nitrate residuals (antisymmetric and symmetric stretching modes at 1468 and 1387 cm^{-1}) and from traces of zinc carbonate (due to the reactions with environmental CO_2) at 900–880 cm^{-1} can be pointed out.

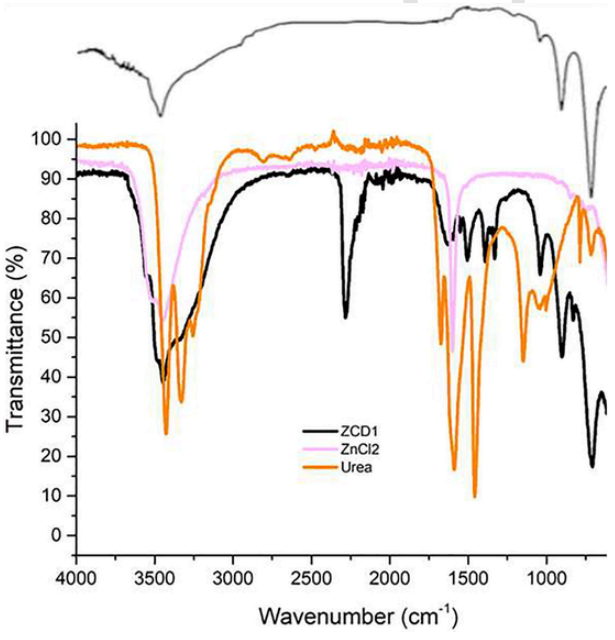

Fig. 3. ZCD1 infrared analysis: Simonkolleite mineral (top panel), ZCD1 (bottom panel, black), $ZnCl_2$ (bottom panel, magenta), urea, (bottom panel, orange). The top panel image was adapted from ref [62] (L. Sithole et al., Simonkolleite nano-platelets: Synthesis and temperature effect on hydrogen gas sensing properties, Applied Surface Science 258 (2012) 7839–7843 upon permission.

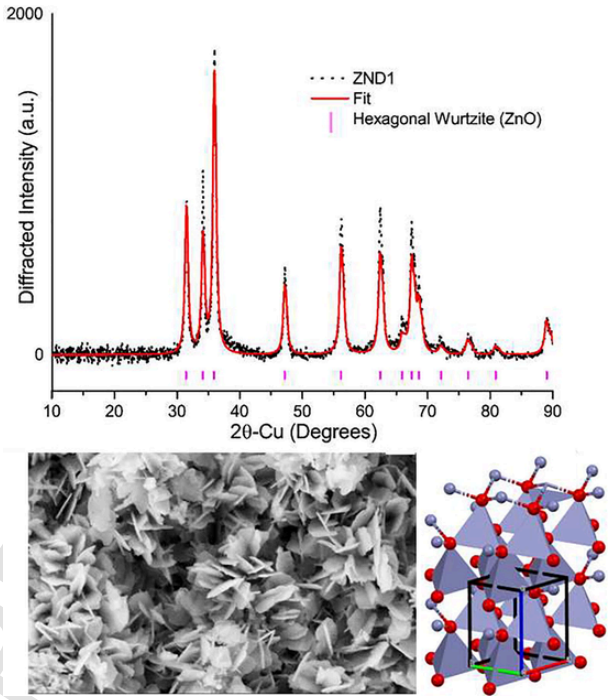

Fig. 4. ZND1 PXRD spectrum (top panel), sample SEM image (bottom panel, left), zincite (ZnO) Wurtzite-type crystal structure (bottom panel, right).

5. Characterization of ZAD1

The XRD pattern measured for ZAD1 is reported in Fig. 6. The profile is quite complex, though some key features can be pinpointed. The peaks originated from ZnO hexagonal Wurtzite structure are visible though they are not the majority contribution to the spectrum. The reflections of pure urea [71] and di-hydrated zinc acetate [72], the two components of the DES reaction medium, seem to contribute to the spectrum, though a proper fit could not be attained. A temptative composition assignment from the fit, based on the presence of unreacted

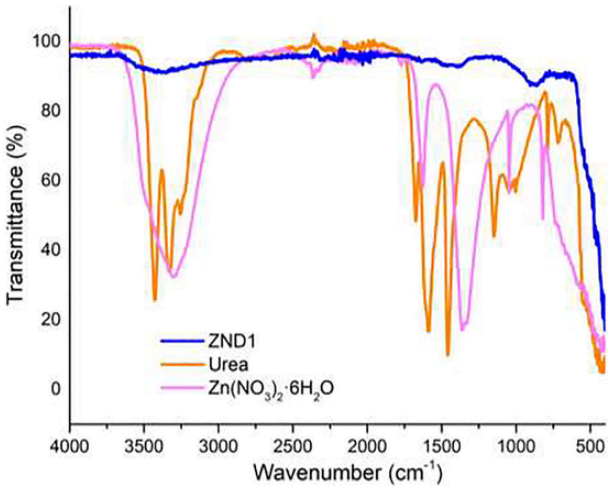

Fig. 5. ZND1 infrared analysis: ZND1, blue; zinc nitrate hexahydrate, magenta; urea, orange.

species, would be ZnO 58 %, 30 % acetate and 12 % urea. Yet, a further analysis could help in the elucidation of this complex pattern. Though numerical data are not availaible, from the visual comparison of the published PXRD spectra of zinc hydroxy acetate/ZnO mixtures (fig. S7 of the paper by Moezzi et al describing the transformation of ZHA (zinc hydroxy acetate, $Zn_5(OH)_8(CH_3CO_2)_2{\cdot}2H_2O$) into ZnO [60], that is reported in Fig. 6, central panel)), with ZAD1 pattern it appears evident that the two spectra share several features, namely the peaks at 12 and 15°, as well as the series of peaks falling around 18, 23, 28 and 38–43°. This point would suggest, therefore, that a non-negligible fraction of ZHA is co-precipitated with ZnO in the solid, together with some urea and acetate residuals. The analysis of ZAD1 IR spectrum (red line of Fig. 7) gives further hints about this complicated composition. Indeed, also for ZAD1 a neat peak appears in the 2200–2300 cm^{-1} region, that could be, again, assigned to urea carbonyl-zinc interactions, like all the pattern in the 1500–900 range which is almost superimposable with that of ZCD1. Furthermore, some key features belonging to the acetate moiety appear, namely the largest wavenumber peak of the very evident double doublet fingerprint (around 1550 cm^{-1}) and the absorption near 620 cm^{-1}, that can be ascribed to carboxylate anion stretching and out-of-plane normal modes [73]. Besides the powder X-ray pattern, also infrared patterns evidence the presence of a sizeable percentage of ZnO in the mixture, considering the Zn-O stretching peak around 500 cm^{-1} that is significantly clearer in ZAD1 than in ZCD1. All these findings seem to support the co-precipitation of different phases when zinc acetate is used as DES component in the reaction conditions examined, i. e. besides the sought--for zinc oxide, large quantities of ZHA and some non-negligible fractions of zinc acetate are found in the nanoparticles. Regarding the microscopy study (Fig. 5, left panel) also ZAD1 seems to be composed of layered platelets typical of LHS/LHD family of compounds, of dimension 200–500 nm, though having edges less sharp than ZCD1. The elemental microanalysis of the particles shows, differently from ZCD1, the presence of N atoms (Fig S5, supplementary material). This would suggest that urea or DES residuals are larger in ZAD1 than in ZCD1, although the infrared spectrum of the latter can be explained only taking into account the presence of additional contributions of *N*-containing fragment, either the DES or residual urea, with respect to simonkolleite mineral pattern that lacks the relative features. The ATR-IR spectra of the three samples are reported together in Fig. 7.

6. Photoluminescence spectra

ZnO is a direct band gap II-VI semiconductor ($E_g \simeq 3.40$ eV) at room temperature, with a large exciton binding energy (around 60 meV). Such electronic features facilitate excitonic stimulated emission and

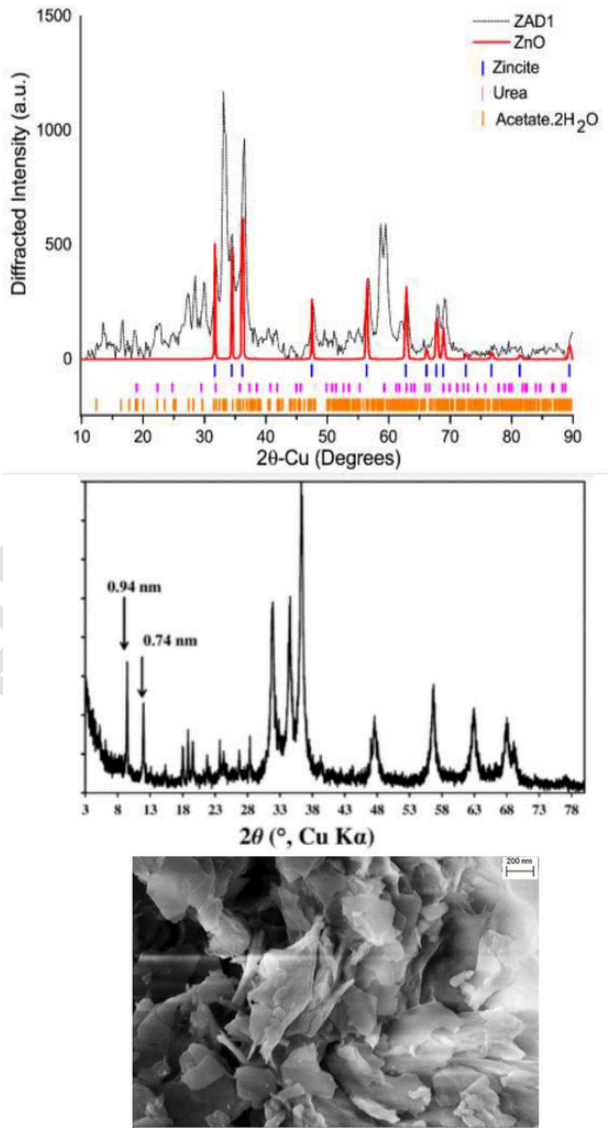

Fig. 6. ZAD1: Measured PXRD spectrum (top panel); Zinc hydroxy acetate/ZnO mixture powder X-ray spectrum (image taken and adapted upon permission from [54], Amir Moezzi, et al, Zinc Hydroxyacetate and Its Transformation to Nanocrystalline Zinc Oxide, Inorg. Chem. 2013, 52, 1, 95–102. Copyright {2013} American Chemical Society (central panel); Sample SEM image (bottom panel).

give origin to a large variety of optical properties, including a near-band-edge emission in the UV region (3.3777 eV / 367 nm) ascribed to free exciton recombination and other broad violet, green, and yellow emission bands [74], which have been ascribed to the interplay of various intrinsic defects, such as zinc and oxygen interstitials (Zni, Oi), oxygen vacancies (Vo), zinc vacancies (VZn), and antisites (OZn) [75]. The positions and intensities of the latter visible emission bands are largely dependent on the size of the nanoparticles/nanocrystals [76], which are obtained following various synthesis routes [77,78], owing to different quantum confinement effects; this issue can be profitably exploited to tune the emission with the aim of producing optical devices of technological interest. Regarding the synthesized solids, that are all white under the solar light, when they are observed with the naked eye while irradiated with a 365 nm UV lamp, an intense yellow luminescence is observed for ZND1, a less intense yellow flare comes from ZAD1, while ZCD1 shows a feeble bluish-white emission (Fig. 8). Therefore, to give further insight on the possibility of using of using ZCD1, ZND1 and ZAD1 as fluorescence probes, we investigated the emission

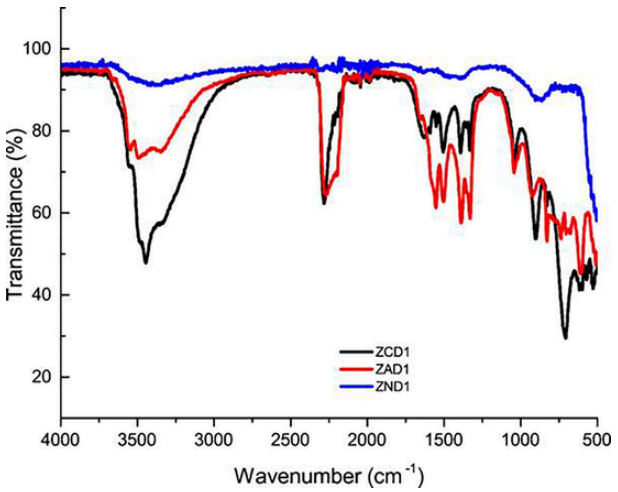

Fig. 7. ATR infrared spectra of the samples. ZND1: blue line, ZCD1: black line; ZAD1: red line.

Fig. 8. Photoluminescence of the three solid samples. ZND1: left; ZAD1: center; ZCD1: right. The excitation was performed with a 365 nm UV lamp.

spectra of their ethanol dispersions, using a 330 nm excitation beam. The results of the measurements are shown in Fig. 9. As it can be seen, all the three systems have a violet fluorescence peak around 420 nm (ZCD: 419, ZND1: 421, ZAD1: 422), while in ZND1 and ZAD1 the distribution is bimodal, the former having an intense emission band centered at 577 nm (yellow) while the latter shows an evident shoulder in the 500–700 nm range. Almost no intensity can be observed for ZCD1 in that region. The blue-violet or bluish-white emission has been reported in the literature for other minerals having layered structure [79], like

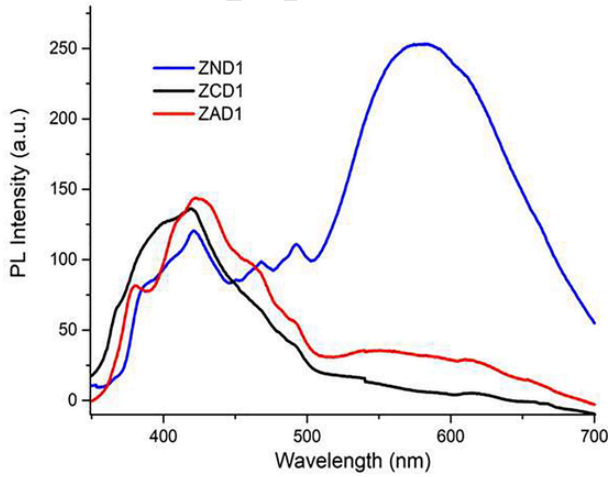

Fig. 9. Photoluminescence spectra of the synthesized samples in ethanol dispersion (1 mg/mL) under 330 nm excitation (Xe lamp).

the forefather brucite $Mg(OH)_2$ [80] or the zinc-containing hydroxyzincite $Zn_5(CO_3)_2(OH)_6$ [81]. The luminescence data obtained from ethanol dispersion comply satisfactorily with the colors observed by the eye in the solids, considering the possible effect of the solvent on the emission [82].. TThe study will be further extended by including more quantitative photoluminescence measurements on solid samples and will be reported in a forthcoming paper.

7. Conclusions

In this work, we have reported for the first time the synthesis of zinc oxide nanoparticles in Type-IV DES. The liquid phases are easily obtained by simply mixing the zinc salt with urea in 1:3.54 ratio under stirring. Heating the mixture to 85 °C was required for zinc acetate, while the other two zinc salts considered (zinc chloride and zinc nitrate) lead to DES liquid around room temperature. The method described appears to be a convenient way to introduce the metal in the system directly, without requiring addition of metal salt to the DES before the precipitation. In the three cases considered, the product formation was accomplished by adding solid NaOH to the DES mixture under stirring at the lowest possible temperature at which the mixture remained liquid. Three different solid systems were synthesized: high purity ZnO nanometrical layered particles were prepared using $Zn(NO_3)_2$; zinc hydroxychloride nanoparticles were obtained from $ZnCl_2$:urea DES, whereas a complex mixture containing both zinc oxide and zinc hydroxy acetate was formed using zinc acetate as DES component. Compared to the nanoparticles obtained in water with other low-temperature or "green" methods, that lead to spherical nanoparticles, the new procedure described for zinc nitrate DES allows the obtainment of layered ZnO nano-platelets in a very straightforward manner, with no need of complex procedures. An added value of the obtained NPs is their quite strong yellow photoluminescence, which could pave the way for their use as fluorescent probes.

Further investigations on this subject are planned, in order to assess if the use of other non-basic anions as DES IV components (except chloride, that has proved to be inappropriate, given the strong tendency of forming oxychloride salts), like, for instance, sulphate, perchlorate, trifluorosulphonate, etc can be employed to prepare ZnO and/or other metal oxide nanoparticles of desired morphology. Exploration of HBD different than urea is envisaged. Further studies on the effect of nanoparticle morphology on the photoluminescence properties of these systems are planned, in order to tune the emission wavelengths, the intensity and the temperature response, with the final aim of developing and optimizing the employment of these nanoparticle systems in the field of sensoristics.

Funding

This research was funded by Regione Lazio within the call n. G04014-13/04/2021 "Progetti di Gruppi di Ricerca 2020", Grant No A0375-2020-36643-Sviluppo di un Dispositivo Portatile Integrato per la Valutazione Spettroscopica Multimodale non Invasiva della Qualità di Materie Prime Alimentari (B85F21001350002).

CRediT authorship contribution statement

Lorenzo Gontrani : Conceptualization, Methodology, Investigation, Writing – original draft, Writing – review & editing. **Domenica Tommasa Donia :** Visualization, Investigation. **Elvira Maria Bauer :** Investigation, Validation. **Pietro Tagliatesta :** Supervision, **Marilena Carbone :** Visualization, Funding acquisition, Supervision, Writing - review & editing.

Declaration of Competing Interest

The authors declare that they have no known competing financial interests or personal relationships that could have appeared to influence the work reported in this paper.

Data availability

Data will be made available on request.

Acknowledgments

The assistance of Cadia D' Ottavi and Prof. Olga Russina (XRD spectra), Dr. Francesco Mura (SEM images), Prof. A. Porchetta and Dr. A. Chamorro (chemiluminescence) is acknowledged. LG thanks Dr. Matteo Bonomo (University of Turin) for the fruitful discussions and suggestions.

Appendix A. Supplementary data

Supplementary data to this article can be found online at https://doi.org/10.1016/j.ica.2022.121268.

References

[1] A.B. Djurišić, X. Chen, Y.H. Leung, A. Man Ching Ng, J. Mater. Chem. 22 (2012) 6526.
[2] J. Wang, R. Chen, L. Xiang, S. Komarneni, Ceram. Int. 44 (2018) 7357–7377.
[3] L. Guo, Y. Shi, X. Liu, Z. Han, Z. Zhao, Y. Chen, W. Xie, X. Li, Biosens. Bioelectron. 99 (2018) 368–374.
[4] L. Goris, R. Noriega, M. Donovan, J. Jokisaari, G. Kusinski, A. Salleo, J. Electron. Mater. 38 (2009) 586–595.
[5] Y.J. Lu, Z.F. Shi, C.X. Shan, D.Z. Shen, in: Nanoscale Semiconductor Lasers, Elsevier, 2019, pp. 75–108.
[6] C.C. Li, Z.F. Du, L.M. Li, H.C. Yu, Q. Wan, T.H. Wang, Appl. Phys. Lett. 91 (2007) 032101.
[7] J. Liqiang, W. Baiqi, X. Baifu, L. Shudan, S. Keying, C. Weimin, F. Honggang, J. Solid State Chem. 177 (2004) 4221–4227.
[8] Y.-B. He, G.-R. Li, Z.-L. Wang, C.-Y. Su, Y.-X. Tong, Energy Environ. Sci. 4 (2011) 1288.
[9] D.-Y. Son, J.-H. Im, H.-S. Kim, N.-G. Park, The Journal of Physical Chemistry C 118 (2014) 16567–16573.
[10] X. Wang, F. Sun, Y. Duan, Z. Yin, W. Luo, Y. Huang, J. Chen, J. Mater. Chem. C Mater. 3 (2015) 11397–11405.
[11] K.M. Lee, C.W. Lai, K.S. Ngai, J.C. Juan, Water Res. 88 (2016) 428–448.
[12] C.B. Ong, L.Y. Ng, A.W. Mohammad, Renew. Sustain. Energy Rev. 81 (2018) 536–551.
[13] S.H. Ammar, W.A. Abdulnabi, H.D.A. Kader, Environ. Nanotechnol. Monit. Manag. 13 (2020).
[14] M. Carbone, R. Briancesco, L. Bonadonna, Environ. Nanotechnol. Monit. Manag. 7 (2017) 97–102.
[15] D.T. Donia, M. Carbone, Int. J. Environ. Sci. Technol. 16 (2019) 583–600.
[16] M. Carbone, E. Maria Bauer, L. Micheli, M. Missori, Colloids Surf. A Physicochem. Eng. Asp 532 (2017) 178–182.
[17] M. Carbone, M. Missori, L. Micheli, P. Tagliatesta, E.M. Bauer, Materials 13 (2020) 1417.
[18] M. Carbone, A. Nesticò, N. Bellucci, L. Micheli, G. Palleschi, Electrochim. Acta 246 (2017) 580–587.
[19] M. Carbone, Appl. Sci. 10 (2020) 6251.
[20] M. Carbone, P. Tagliatesta, Materials 13 (2020) 1880.
[21] S. Babazadeh, R. Bisauriya, M. Carbone, L. Roselli, D. Cecchetti, E.M. Bauer, S. Sennato, P. Prosposito, R. Pizzoferrato, Sensors 21 (2021) 6353.
[22] L. Gontrani, O. Pulci, M. Carbone, R. Pizzoferrato, P. Prosposito, Molecules 26 (2021) 5519.
[23] F. Limosani, E.M. Bauer, D. Cecchetti, S. Biagioni, V. Orlando, R. Pizzoferrato, P. Prosposito, M. Carbone, Nanomaterials 11 (2021) 2249.
[24] M. Carbone, Appl. Sci. 12 (2022) 2839.
[25] D.T. Donia, E.M. Bauer, M. Missori, L. Roselli, D. Cecchetti, P. Tagliatesta, L. Gontrani, M. Carbone, Symmetry (Basel) 13 (2021) 733.
[26] E.L. Smith, A.P. Abbott, K.S. Ryder, Chem. Rev. 114 (2014) 11060–11082.
[27] A. Abo-Hamad, M. Hayyan, M.A. AlSaadi, M.A. Hashim, Chem. Eng. J. 273 (2015) 551–567.
[28] B.B. Hansen, S. Spittle, B. Chen, D. Poe, Y. Zhang, J.M. Klein, A. Horton, L. Adhikari, T. Zelovich, B.W. Doherty, B. Gurkan, E.J. Maginn, A. Ragauskas, M. Dadmun, T.A. Zawodzinski, G.A. Baker, M.E. Tuckerman, R.F. Savinell, J.R. Sangoro, Chem. Rev. 121 (2021) 1232–1285.
[29] D.V. Wagle, H. Zhao, G.A. Baker, Acc. Chem. Res. 47 (2014) 2299–2308.
[30] L. Gontrani, P. Tagliatesta, D.T. Donia, E.M. Bauer, M. Bonomo, M. Carbone, Molecules 27 (2022) 2045.
[31] M. Bonomo, L. Gontrani, A. Capocefalo, A. Sarra, A. Nucara, M. Carbone, P. Postorino, D. Dini, J. Mol. Liq. 319 (2020) 114292.
[32] M.C. Gutiérrez, D. Carriazo, C.O. Ania, J.B. Parra, M.L. Ferrer, F. del Monte, Energy Environ. Sci. 4 (2011) 3535.
[33] M. Busato, V. di Lisio, A. del Giudice, P. Tomai, V. Migliorati, L. Galantini, A. Gentili, A. Martinelli, P. D'Angelo, J. Mol. Liq. 331 (2021) 115747.
[34] S. Kaur, M. Kumari, H.K. Kashyap, J. Phys. Chem. B 124 (2020) 10601–10616.
[35] L. Gontrani, M. Bonomo, N. v. Plechkova, D. Dini, R. Caminiti, PCCP 20 (2018) 30120–30124.
[36] L. Gontrani, N.V. Plechkova, M. Bonomo, ACS Sustain. Chem. Eng. (2019) acssuschemeng.9b02402.
[37] A.P. Abbott, G. Capper, S. Gray, ChemPhysChem 7 (2006) 803–806.
[38] M. Campetella, A. le Donne, M. Daniele, L. Gontrani, S. Lupi, E. Bodo, F. Leonelli, J. Phys. Chem. B 122 (2018) 2635–2645.
[39] A.P. Abbott, G. Capper, D.L. Davies, R.K. Rasheed, V. Tambyrajah, Chem. Commun. (2003) 70–71.
[40] T.K. Dang, N. van Toan, C.M. Hung, N. van Duy, N.N. Viet, L.V. Thong, N.T. Son, N. van Hieu, T. le Manh, J. Appl. Electrochem. 52 (2022) 299–309.
[41] H. Jia, J. Sun, M. Dong, H. Dong, H. Zhang, X. Xie, Nanoscale 13 (2021) 19004–19011.
[42] T.N.J.I. Edison, R. Atchudan, N. Karthik, S. Chandrasekaran, S. Perumal, P.B. Raja, V. Perumal, Y.R. Lee, Fuel 297 (2021) 120786.
[43] Y. Hou, Z. Peng, J. Liang, M. Liu, Surf. Coat. Technol. 405 (2021) 126587.
[44] J.D. Mota-Morales, M.C. Gutiérrez, M.L. Ferrer, R. Jiménez, P. Santiago, I.C. Sanchez, M. Terrones, F. del Monte, G. Luna-Bárcenas, J Mater Chem A Mater 1 (2013) 3970.
[45] C. Gu, H. Zhang, X. Wang, J. Tu, Mater. Res. Bull. 48 (2013) 4112–4117.
[46] J.N. Baby, B. Sriram, S.-F. Wang, M. George, ACS Sustain Chem Eng 8 (2020) 1479–1486.
[47] Y. Zhang, J. Ru, Y. Hua, P. Huang, J. Bu, Z. Wang, Mater. Lett. 283 (2021) 128742.
[48] L. Das, L.D. Koonathan, A. Kunwar, S. Neogy, A.K. Debnath, S. Adhikari, Mater Adv 2 (2021) 4303–4315.
[49] S. Taghavi, A. Amoozadeh, F. Nemati, J. Chem. Technol. Biotechnol. 96 (2021) 384–393.
[50] S. Taghavi, A. Amoozadeh, F. Nemati, Appl. Organomet. Chem. 35 (2021).
[51] T.T. Nguyen, P.H. Tran, RSC Adv. 10 (2020) 9663–9671.
[52] H. Lian, S. Hong, A. Carranza, J.D. Mota-Morales, J.A. Pojman, RSC Adv. 5 (2015) 28778–28785.
[53] A.P. Abbott, J.C. Barron, K.S. Ryder, D. Wilson, Chem. A Eur. J. 13 (2007) 6495–6501.
[54] E.I. Eweka, D.H. Kerridge, Chem. Pap. 53 (1999) 11–15.
[55] A. Mackowiak, P. Galek, K. Fic, ChemElectroChem 8 (2021) 4028–4037.
[56] L. Adhikari, N.E. Larm, G.A. Baker, ACS Sustain. Chem. Eng. 7 (2019) 11036–11043.
[57] Z. Meng, Y. Zhang, Q. Zhang, X. Chen, L. Liu, S. Komarneni, F. Lv, Appl. Surf. Sci. 396 (2017) 799–803.
[58] G. Arizaga, K. Satyanarayana, F. Wypych, Solid State Ion 178 (2007) 1143–1162.
[59] T. Hongo, T. Iemura, S. Satokawa, A. Yamazaki, Appl. Clay Sci. 48 (2010) 455–459.
[60] A. Moezzi, A. McDonagh, A. Dowd, M. Cortie, Inorg. Chem. 52 (2013) 95–102.
[61] F.C. Hawthorne, E. Sokolova, Can. Mineral. 40 (2002) 939–946.
[62] J. Sithole, B.D. Ngom, S. Khamlich, E. Manikanadan, N. Manyala, M.L. Saboungi, D. Knoessen, R. Nemutudi, M. Maaza, Appl. Surf. Sci. 258 (2012) 7839–7843.
[63] F. Zhu, D. Persson, D. Thierry, C. Taxen, Corrosion 56 (2000) 1256–1265.
[64] C.A. Sorrell, J. Am. Ceram. Soc. 60 (1977) 217–220.
[65] A.C. Holland, An Investigation into the Three Component System, Zinc Oxide, Hydrochloric Acid, Zinc Chloride and Water, 1928.
[66] A.P. Abbott, G. Capper, D.L. Davies, K.J. McKenzie, S.U. Obi, J. Chem. Eng. Data 51 (2006) 1280–1282.
[67] A.P. Abbott, G. Capper, D.L. Davies, R.K. Rasheed, P. Shikotra, Inorg. Chem. 44 (2005) 6497–6499.
[68] B.H. Toby, R.B. von Dreele, J. Appl. Crystallogr. 46 (2013) 544–549.
[69] D. Peña-Solórzano, V. v. Kouznetsov, C. Ochoa-Puentes, New J. Chem. 44 (2020) 7987–7997.
[70] R.T. Downs, M. Hall-Wallace, Am. Mineral. 88 (2003) 247–250.
[71] Cambridge Crystallographic Data Center (CCDC) structure 131762 – UREAXX02 (1999).
[72] Cambridge Crystallographic Data Center (CCDC) structure 128994 (1997).
[73] T. Ishioka, Y. Shibata, M. Takahashi, I. Kanesaka, Y. Kitagawa, K.T. Nakamura, Spectrochim Acta A Mol Biomol Spectrosc 54 (1998) 1827–1835.
[74] A.K. Singh, S.K. Singh, in: Nanostructured Zinc Oxide, Elsevier, 2021, pp. 189–208.
[75] M.D. McCluskey, S.J. Jokela, J. Appl. Phys. 106 (2009) 071101.
[76] L. Irimpan, V.P.N. Nampoori, P. Radhakrishnan, A. Deepthy, B. Krishnan, J. Appl. Phys. 102 (2007) 063524.
[77] L. Kumar Jangir, Y. Kumari, A. Kumar, M. Kumar, K. Awasthi, Mater. Chem. Front. 1 (2017) 1413–1421.
[78] J.A. Kannan, K. Balasubramanian, Appl. Phys. A 126 (2020) 602.
[79] Y. Zhou, X. Li, K. Wang, F. Hu, C. Zhai, X. Wang, J. Bai, J. Alloy. Compd. 770 (2019) 6–16.
[80] T. Ramesh, A. Taj, Internatioinal Journal of Science Research (2013) 487–494.
[81] M. Robbins, Fluorescence: Gems and Minerals Under Ultraviolet Light, Geoscience Press, 1994.
[82] N.C. Horti, M.D. Kamatagi, N.R. Patil, M.N. Wari, S.R. Inamdar, Optik (Stuttg)

169 (2018) 314–320.